

To appear in AJ, May 2001

Color Transformations for the 2MASS Second Incremental Data Release

John M. Carpenter

California Institute of Technology, Department of Astronomy, MS 105-24,
Pasadena, CA 91125; email: jmc@astro.caltech.edu

ABSTRACT

Transformation equations are presented to convert colors and magnitudes measured in the AAO, ARNICA, CIT, DENIS, ESO, LCO (Persson standards), MSSSO, SAAO, and UKIRT photometric systems to the photometric system inherent to the 2MASS Second Incremental Data Release. The transformations have been derived by comparing 2MASS photometry with published magnitudes and colors for stars observed in these systems. Transformation equations have also been derived indirectly for the Bessell & Brett (1988) and Koornneef (1983) homogenized photometric systems.

Subject headings: standards — infrared: stars

1. Introduction

The 2 Micron All Sky Survey (2MASS) will provide J , H , and K_s band photometry for millions of galaxies and nearly a half billion stars. While the 2MASS data alone will make important contributions to many fields of study, the scientific impact of many programs can be further enhanced by comparing 2MASS photometry with existing photometric measurements or by conducting follow-up observations. One difficulty in directly comparing 2MASS photometry with other near-infrared observations is that these comparison data will often be obtained with a set of filters that have different transmissions profiles and effective wavelengths than the filters adopted for the 2MASS survey. Variations in the filter transmission characteristics can lead to systematic differences in the observed stellar colors, especially for objects with extremely red spectral energy distributions or unusual spectral line features. Any detailed comparisons between 2MASS data and observations conducted at other telescopes then requires that both sets of photometry be placed on a common photometric system. Since 2MASS will provide photometry for sources over the entire sky, it is natural to adopt the 2MASS photometric system as the reference point for these comparisons.

As the 2MASS survey has progressed, subsets of the survey data have been publicly released on three occasions to date. The 2MASS Second Incremental Release in particular provides photometry for both point and extended sources for $\approx 47\%$ of the sky. Even though these catalogs are considered preliminary, as all data will be reprocessed at the completion of the 2MASS observations with a

final version of the data reduction pipeline, the data contained in the Second Incremental Release already meets a high degree of global photometric uniformity (Nikolaev et al. 2000). It is therefore appropriate to determine the color transformations between the 2MASS Second Incremental Release and other photometric systems. In this paper, I derive these transformation equations using 2MASS observations of the standard stars that define commonly used photometric systems. This exercise necessarily emphasizes recent grids of faint near-infrared standards (Casali & Hawarden 1992; Carter & Meadows 1995; Hunt et al. 1998; Persson et al. 1998) which have effectively replaced more traditional standards (Glass 1974; Elias et al. 1982; Allen & Cragg 1983; Carter 1990; Bouchet, Manfroid, & Schmider 1991; McGregor 1994) that are usually too bright to be observed with modern instrumentation. The 2MASS data analyzed in this study are summarized in Section 2. Section 3 examines the internal consistency of the 2MASS photometry, the temporal stability of the 2MASS photometric system, and the color transformations between the northern and southern 2MASS surveys. The color transformations between 2MASS and other photometric systems are then presented in Section 4.

2. 2MASS Photometry

The 2MASS observations are being conducted using 1.3 meter telescopes at Mt. Hopkins in Arizona (the Northern survey) and at Cerro Tololo in Chile (the Southern survey). Data from both telescopes are processed, calibrated, and analyzed for quality control at the Infrared Processing and Analysis Center (IPAC). The 2MASS photometry analyzed in this study has been obtained from the internal 2MASS working databases at IPAC that contain both the 2MASS Second Incremental Data Release and photometry for the remaining part of the sky observed to date. Further, all but one of the 2MASS calibration fields are centered on standard stars contained in Persson et al. (1998) and Casali & Hawarden (1992), and wherever possible, the more accurate, globalized 2MASS magnitudes for stars in these regions computed by Nikolaev et al. (2000) have been adopted. These additional data are included in this analysis to increase the number of standard stars with 2MASS photometry and allow correspondingly more accurate color transformations to be derived. While these additional data meet the photometric requirements used to generate the Second Incremental Release catalogs, they may not necessarily satisfy other requirements adopted for this release as described in the 2MASS Explanatory Supplement (Cutri et al. 2000). (For example, the Second Incremental Release required that all tiles must be part of a block of at least 3 contiguous tiles in right ascension, a requirement not imposed here.) Further, it should be noted that the data calibration procedures have evolved as the 2MASS survey has progressed, and the derived transformations presented in this paper should be regarded as preliminary until the 2MASS data are reprocessed in a uniform manner at the completion of survey operations. In practice, any changes in the calibration over the course of the survey to date have been $\lesssim 0.01^m$ (Nikolaev et al. 2000; see also Section 3).

The 2MASS Explanatory Supplement (Cutri et al. 2000) describes the Second Incremental Release in detail, and only relevant aspects of the data processing from this document are summarized here. Photometry for bright stars ($\approx 5\text{-}9^m$) are measured in the 2MASS data reduction pipeline using a circular aperture on a sequence of six 51 ms integration images. Stars brighter than $\approx 5^m$ are saturated even in these short exposures and accurate magnitudes cannot be derived. Magnitudes for fainter stars were obtained using Point Spread Function (PSF) fitting photometry on six, 1.3 s integration images. The photometric uncertainty for stars measured with aperture photometry is computed from the standard deviation of the mean of the six aperture magnitudes. For PSF fitting photometry, the photometric uncertainty is derived from the Poisson noise associated with the observed flux and the fluctuations in the sky background as measured in a sky annulus around each star. The normalization to remove any potential systematic difference between the PSF and aperture photometry is discussed in the 2MASS Explanatory Supplement (Cutri et al. 2000). In addition to the internal photometric accuracy, a zero-point uncertainty is determined from calibration fields observed every hour during survey operations. (For early survey operations, the calibration fields were observed every 2 hours.) The total photometric uncertainty adopted here is the quadrature sum of the zero-point and internal photometric uncertainties for each star. The minimum, total photometric uncertainties in the J , H , and K_s band magnitudes are $\approx 0.02^m$. By comparison, the photometric uncertainties for the standard star observations defining the photometric systems discussed in Section 4 are $\lesssim 0.025^m$ and sometimes less than 0.01^m . Stars in the overlap region between adjacent 2MASS tiles have more than one photometric measurement. While the photometry from only one of these observations appears in the public release Point Source Catalog, these photometric measurements have been averaged here, with each measurement weighted by the inverse square of the total photometric uncertainty.

3. The 2MASS Photometric System

3.1. Filters

Both the Northern and Southern 2MASS telescopes are outfitted with a similar set of optics, filters, and detectors to observe the J , H , and K_s bands simultaneously. Since the total transmission through the atmosphere and the optical elements define any photometric system, it is instructive to review these characteristics as they pertain to 2MASS and note any substantial differences from other photometric systems. Figure 1 shows the transmission as a function of wavelength through the 2MASS optical path, including the telescope mirror reflectivity, the dewar window, anti-reflection coatings, dichroics, filters, and the NICMOS detector quantum efficiency, but excluding the atmosphere. The dominant source of transmission loss through the optical path is the detector quantum efficiency, which is $\approx 0.6\text{-}0.65$ in the J , H , and K_s bandpasses. A model atmospheric transmission for the mean conditions at Mt. Hopkins is shown separately in Figure 1 as indicated by the thin solid line. The atmospheric transmission data, kindly provided by Martin Cohen, was computed using the USAF PLEXUS code and binned to a resolution of $0.002\mu\text{m}$ for display

purposes. The transmission curves for both the optical elements and the atmosphere are tabulated in the 2MASS Explanatory Supplement (Cutri et al. 2000).

The primary distinction between 2MASS and many other photometric systems is that the 2MASS K_s filter transmission was specially designed to cut off at $\approx 2.3\mu\text{m}$ in order to reduce the noise contribution from the thermal background. In this manner, the noise in the K_s -band observations will be less sensitive to variations in the ambient temperature, allowing for a more uniform photometric survey. A similar filter has been adopted by the DENIS survey (Epchtein et al. 1999) and also was incorporated into the standard star observations by Persson et al. (1998). By comparison, more traditional Johnson K filters have significant transmission out to $\approx 2.4\mu\text{m}$. Therefore, throughout this paper, the 2MASS K_s (“K-short”) filter is distinguished from the Johnson K filter when presenting the color transformations.

As shown in Figure 1, the short and long wavelength cutoff of the 2MASS J -band filter extends into the atmospheric H_2O absorption features at $\approx 1.1\mu\text{m}$ and $1.4\mu\text{m}$. In dry weather, the transmission at these wavelengths can be significant compared to typical conditions, implying that the effective J -band wavelength, calibration zero-points, and possibly color transformations will depend on the atmospheric water vapor content. Indeed, the J -band calibration zero-points often show smooth variations within a night as large as 0.1 magnitudes (Cutri et al. 2000), and seasonal variations in the average zero-point as large as 0.2 magnitudes are observed. The H - and K_s -band zero-points are relatively constant within a night, although seasonal variations of ≈ 0.1 magnitudes are observed. While the 2MASS survey does not record the atmospheric water vapor content directly, these zero-point variations are presumably due to changes in the amount of water vapor.

The above discussion indicates that various aspects of 2MASS photometry need to be investigated before deriving the color transformations between 2MASS and other photometric systems, namely, (1) the temporal stability of the 2MASS photometric system over the 3+ years of survey operations; (2) the effects of the atmospheric water vapor content on the color transformations, in particular those involving J -band; and (3) any differences in the photometric systems between the Northern and Southern surveys. Nikolaev et al. (2000) have discussed these issues in terms of the global magnitude calibration of the 2MASS survey and found that any temporal changes in the global calibration of the J , H , and K_s magnitudes in the 2MASS survey are $\lesssim 0.01^m$. However, since most of the standard stars analyzed by Nikolaev et al. (2000) span a small range of colors, the stability of the 2MASS photometric system as pertaining to the stellar colors remains to be established. The following subsections present such an analysis, and it is shown that any internal variations in the 2MASS color transformations are less than the photometric uncertainties for any individual star.

3.2. Temporal Stability

To examine any possible temporal variations in the observed stellar colors, 2MASS photometry in a $\approx 1^\circ \times 6^\circ$ region near the Galactic plane was analyzed that has been observed on two occasions with the Mt. Hopkins telescope, once on June 12, 1997 near the start of Northern survey operations, and again on May 24, 2000. Thus comparison of these sets of observations will indicate any change in the photometry over nearly a 3 year time period. Besides the long time baseline, this field was chosen since the J -band calibration zero-point on the two nights is the same to within 0.01^m , suggesting that the atmospheric conditions were similar for both sets of observations (see Section 3.1). A similar sized region with large differences in the J -band zero-points is analyzed in the following section.

Sources were selected from both survey nights that satisfied the following criteria: (1) the source is free of any flags from the 2MASS data processing pipeline that indicate the photometry may be contaminated by a nearby star; and (2) if the magnitudes were computed using PSF fitting photometry, the reduced chi-squared from the PSF fit is ≤ 2.0 to eliminate any potentially extended sources. Point sources in the first night of observations that satisfy these criteria and contain a signal to noise ratio ≥ 15 in each of the J , H , and K_s bands were matched with a source in the second observational set using a $1''$ search radius. A total of 34,083 sources were matched in this manner. The absolute value of the average photometric offset between the two nights, computed by averaging the difference in photometry for all matched sources, is 0.025^m , 0.001^m , and 0.002^m at J , H , and K_s band respectively. Measured relative to the zero-point calibration uncertainties, the offsets are 0.8σ , 0.04σ , and 0.09σ . Therefore, any difference in the photometric zero-points between the two nights is within the nightly zero-point uncertainties. The zero-point offsets were removed by adding a constant to the first night of observations such that the following analysis compares only the difference of the stellar colors. No offsets have been applied to the 2MASS data, however, when comparing the 2MASS photometry with other photometric systems.

Linear fits to the $J - K$, $J - H$, and $H - K$ colors between the two sets of observations were performed using the FITEXY program (Press et al. 1992) that incorporates uncertainties from both measurements. The reduced chi-squared is ≈ 0.7 for each of the fits, indicating that the colors are well modeled by a linear relation and that the residuals are consistent with random noise. Based on the fit, the difference in the observed colors between observations taken ≈ 3 years apart is less than 0.01^m for $J - H < 1.3$ and $J - K_s < 1.8$. The results for the $H - K_s$ fit are not meaningful since the observed dispersion in the colors (0.089^m) is only slightly larger than the expected dispersion (0.066^m) due to photometric noise, such that there is little intrinsic variations in the $H - K_s$ colors for this field. Nevertheless, the strong similarity between the $J - H$ and $J - K_s$ colors suggest that any intrinsic variations in the $H - K_s$ colors must also be small. Thus any temporal changes in the 2MASS color system as judged from the $J - H$ and $J - K_s$ results are comparable to the minimum photometric uncertainties ($\approx 0.02^m$) for any individual star.

3.3. Atmospheric Conditions

As discussed in Section 3.1, the effective transmission through the 2MASS J -band filter depends on the amount of atmospheric water vapor. Variations in the water vapor content may lead to changes in the J -band zero-point calibration and possibly introduce additional color terms for the survey data. To quantify this effect, 2MASS photometry for another $\approx 1^\circ \times 6^\circ$ region was analyzed that has been observed on 2 occasions by the Northern survey telescope in which the J -band zero-point between the 2 nights differed by 0.16^m , presumably due to differences in atmospheric water vapor content. A total of 49,389 stars were identified between the two observations using the criteria described in Section 3.2. The average photometric offsets between the two observations measured relative to the zero-point calibration uncertainties are 0.5σ , 1.1σ , and 1.6σ for J , H , and K_s respectively. Thus the photometric offsets were consistent within the calibration uncertainties, and the zero-point differences were removed before comparing the near-infrared colors (see Section 3.2). The reduced chi-squared is ≈ 0.9 for each of the linear fits to the near-infrared colors, again indicating that the correlation between the two sets of observations is well represented by a linear relation. Based on the fits, the difference in the observed colors between the two observations is less than 0.014^m for $J - H < 3.2$, less than 0.021^m for $J - K_s < 4.7$, and less than 0.01^m for $H - K_s < 1.5$. Thus no significant change relative to the photometric uncertainties for an individual star was found in the 2MASS photometric system in varying atmospheric conditions.

3.4. Comparison between the 2MASS South and 2MASS North Surveys

While much effort has been placed on making the Northern and Southern operations as identical as possible, small differences in the color systems between the two surveys may still potentially exist. Any differences in the observed stellar colors between the northern and southern hemisphere surveys have been evaluated using 5 fields with declinations between -9° and $+3^\circ$ that were observed by both telescopes between November 1998 and July 2000. A total of 155,011 point sources were matched between the northern and southern survey data using the criteria described in Section 3.2. The average photometric offset, where the offset is in the sense of the magnitude observed in the north minus the magnitude observed from the south, ranges from -0.011^m to 0.039^m among the three bands. Measured relative to the nightly 1σ zero-point calibration uncertainties, the offsets range from -0.45σ to 1.9σ . These photometric zero-point offsets for the 5 fields are within the uncertainties of the nightly calibration, and the offsets have been applied to the northern data on a night-by-night basis. Figure 2 compares the observed $J - K_s$, $J - H$, and $H - K_s$ colors from the northern and southern survey telescopes. In each figure, the contours represent the density of points in the particular diagram, and the dashed line indicates the expected relation if the near-infrared colors are equal. The derived linear relation between the two observations are

$$(J - K_s)_{\text{North}} = (1.000 \pm 0.001)(J - K_s)_{\text{South}} + (-0.001 \pm 0.001) \quad (1)$$

$$(J - H)_{\text{North}} = (1.002 \pm 0.001)(J - H)_{\text{South}} + (-0.003 \pm 0.001) \quad (2)$$

$$(H - K_s)_{\text{North}} = (1.009 \pm 0.001)(H - K_s)_{\text{South}} + (-0.001 \pm 0.001), \quad (3)$$

where the reduced chi-squared from each of the fits is ≈ 0.9 . These equations indicate that the $J - K_s$ and $J - H$ colors from the Northern and Southern surveys are statistically indistinguishable. The slope in the $H - K_s$ transformation, if significant, implies that the maximum $H - K_s$ color difference between the northern and southern survey data over the range of colors shown in Figure 2 is 0.012^{m} , which is within the nightly calibration uncertainties for any individual star. Therefore, in the remainder of this paper, it is assumed that the 2MASS North and South colors systems are identical.

4. Color Transformations

Table 1 summarizes the photometric systems analyzed in the paper. Included in the table are the references to the photometry that defines these systems and the number of stars with available 2MASS photometry at the time of this study that were used to derive the color transformations. Tables containing the 2MASS and published photometry for the individual stars can be found in the 2MASS Explanatory Supplement (Cutri et al. 2000). Notable omissions from this analysis include the homogenized photometric systems put forth by Bessell & Brett (1988) and Koornneef (1983). The Bessell & Brett (1988) system is largely based upon the SAAO photometric system established by Glass (1974), while Koornneef (1983) combines the SAAO and Johnson (Johnson et al. 1966) systems. Both the Johnson and Glass standards are saturated in the 2MASS images and do not have reliable 2MASS photometry. The transformation equations to these homogenized systems have been derived indirectly as described in the Appendices.

The color transformations between 2MASS and the photometric systems summarized in Table 1 were derived by making a linear fit between the published standard star photometry (or in the case of DENIS, publicly available catalog data) and the 2MASS observations of these stars. The specific variables included in the linear fit are $(K_s)_{\text{2MASS}} - K_{\text{std}}$ vs. $(J - K)_{\text{std}}$, $(J - K_s)_{\text{2MASS}}$ vs. $(J - K)_{\text{std}}$, $(J - H)_{\text{2MASS}}$ vs. $(J - H)_{\text{std}}$, and $(H - K_s)_{\text{2MASS}}$ vs. $(H - K)_{\text{std}}$, where std , treated as the X-variable in the fits, represents the photometry for the appropriate photometric system. The transformation equations were derived using the routine FITEXY (Press et al. 1992) that minimizes the chi-squared between the observations and a straight-line model. The uncertainties in both the 2MASS and published photometry are used to evaluate the chi-squared merit function. After examining the residuals from the fit, sources with large discrepancies between the 2MASS and published photometry were removed and the fit was re-derived. Any sources removed from the analysis are noted below when discussing the results for each photometric system. Table 2 summarizes the goodness-of-fit parameters from the linear fit, including the reduced chi-squared (χ^2_{ν}) of the residuals and the probability (q , $0 \leq q \leq 1$) that the reduced chi-squared can be exceeded by chance for gaussian distributed noise. The larger the value of q , the more likely the residuals are consistent with random noise. Table 2 indicates that with the exception of the DENIS-

2MASS fit (see discussion in Section 4.4), the 2MASS and published photometry are reasonably described by a linear relationship and the residuals can be explained by photometric noise. The residuals for the K -band transformations tend to have larger reduced chi-squared values than that for the color transformations, especially for photometric systems that incorporate very red infrared standards. As discussed by Elias et al. (1983, see also Persson et al. 1998), these red standards tend to be near star forming regions and have a greater probability of being variable stars. If any of the red standards do have low amplitude variability, the magnitude transformations will be most affected since the J , H , and K_s band magnitudes will vary simultaneously and produce smaller color changes.

To emphasize that the derived color transformations are valid only for the colors spanned by the published photometry, Figure 3 shows the range of $J - K$ colors contained in the data analyzed here for each photometric system. The appropriate ranges for the $J - H$ and $H - K$ colors can be obtained from inspection of Figures 4-14. In addition, these transformation equations may not apply for objects that exhibit complex spectral energy distributions (e.g. T dwarfs). For these objects, the transformation equations will be sensitive to the exact spectral features that are within the filter transmission curve.

The results from the linear fits are summarized graphically in Figures 4-14 and are described below for each photometric system. In displaying the results, the data are shown as the difference between the 2MASS and standard star photometry as a function of the standard star photometry in order to emphasize subtle, systematic photometric differences. This implies that the X and Y axes are correlated in the plots, which can create artificial trends with slope of -1.0 if the noise in the data exceeds the dynamic range in colors. This effect was quite apparent in the DENIS-2MASS comparisons since the DENIS data have lower signal to noise typically than the 2MASS photometry. For the DENIS results only, the 2MASS photometry is plotted along the X-axis.

4.1. AAO

Allen & Cragg (1983) present photometric standards for the Anglo-Australian Observatory (AAO). Four of these stars are faint enough to be observed with 2MASS and have available 2MASS photometry. In addition, Elias et al. (1983) obtained photometry for several stars with red near-infrared colors to establish the color transformations between the CIT and AAO photometric systems. While most of these stars are not considered primary standards, they were included here since they have a high photometric accuracy (0.01-0.02^m; Elias et al. 1983). Star cskf-13a in Elias et al. (1983) has been observed twice by 2MASS, and on each occasion the reduced chi-squared from the PSF in each of the J , H , and K_s bands is between 2 and 4. Therefore this object is extended at the 2MASS resolution and has been removed from the linear fit.

Figure 4 shows the correlation between the 2MASS and AAO K -band magnitudes and $J - H$, $H - K$, and $J - K$ colors for the 14 stars with available photometry. The difference in the K -band

magnitudes are shown as a function of the $J - K$ color in this figure to investigate any color terms in the magnitude relations. Two panels are shown for each relation. The top panel presents the observed data, and the bottom panel shows the residuals after subtracting the fit. The derived color transformations are

$$(K_s)_{\text{2MASS}} = K_{\text{AAO}} + (-0.021 \pm 0.008)(J - K)_{\text{AAO}} + (-0.032 \pm 0.012) \quad (4)$$

$$(J - H)_{\text{2MASS}} = (0.924 \pm 0.015)(J - H)_{\text{AAO}} + (0.000 \pm 0.016) \quad (5)$$

$$(J - K_s)_{\text{2MASS}} = (0.943 \pm 0.009)(J - K)_{\text{AAO}} + (0.024 \pm 0.014) \quad (6)$$

$$(H - K_s)_{\text{2MASS}} = (0.974 \pm 0.033)(H - K)_{\text{AAO}} + (0.032 \pm 0.016) \quad (7)$$

4.2. ARNICA

The Arcetri NICMOS3 camera (ARNICA) photometric system is defined by the standard observations of 86 northern hemisphere stars by Hunt et al. (1998; see also Hunt et al. 2000). The calibration of ARNICA system is based on the UKIRT faint standards (Casali & Hawarden 1992). The following stars with available 2MASS photometry were omitted from the linear fit: all five stars in the AS16 group since 3 of the 4 ARNICA standards with the highest residuals are in this field; AS17-4 since higher resolution observations indicate the source is non-stellar and possibly variable (L. Hunt, private communication); AS27-0 (UKIRT FS 24) since it is a variable star (Hawarden et al. 2000); AS29-0 (UKIRT FS 25) and AS31-0 (UKIRT FS 28) since they contain a nearby companion (Hawarden et al. 2000) that may influence the accuracy of the 2MASS photometry. Figure 5 compares the 2MASS and ARNICA photometry for 65 stars. The range of near-infrared colors in the ARNICA standards list is relatively small, especially for $H - K$, and further observations are needed with the ARNICA camera to determine the transformations over a larger range of near-infrared colors. The derived transformations are

$$(K_s)_{\text{2MASS}} = K_{\text{ARNICA}} + (-0.024 \pm 0.011)(J - K)_{\text{ARNICA}} + (0.012 \pm 0.006) \quad (8)$$

$$(J - H)_{\text{2MASS}} = (1.054 \pm 0.020)(J - H)_{\text{ARNICA}} + (-0.025 \pm 0.008) \quad (9)$$

$$(J - K_s)_{\text{2MASS}} = (1.056 \pm 0.016)(J - K)_{\text{ARNICA}} + (-0.018 \pm 0.008) \quad (10)$$

$$(H - K_s)_{\text{2MASS}} = (1.059 \pm 0.070)(H - K)_{\text{ARNICA}} + (0.007 \pm 0.008) \quad (11)$$

4.3. CIT

The Caltech (CIT) photometric system was described by Frogel et al. (1978) and became defined by the standard star observations from Elias et al. (1982). In addition, Elias et al. (1983) obtained photometry in the CIT system for a number of stars with large near-infrared colors.

As noted above, cskf-13a from Elias et al. (1983) has been omitted from this analysis. Figure 6 compares the photometry for 41 stars with CIT and 2MASS measurements. The derived color transformations are

$$(K_s)_{\text{2MASS}} = K_{\text{CIT}} + (0.000 \pm 0.005)(J - K)_{\text{CIT}} + (-0.024 \pm 0.003) \quad (12)$$

$$(J - H)_{\text{2MASS}} = (1.076 \pm 0.010)(J - H)_{\text{CIT}} + (-0.043 \pm 0.006) \quad (13)$$

$$(J - K_s)_{\text{2MASS}} = (1.056 \pm 0.006)(J - K)_{\text{CIT}} + (-0.013 \pm 0.005) \quad (14)$$

$$(H - K_s)_{\text{2MASS}} = (1.026 \pm 0.020)(H - K)_{\text{CIT}} + (0.028 \pm 0.005) \quad (15)$$

4.4. DENIS

The DENIS survey has released preliminary I , J , and K_s band photometry for $\approx 2\%$ of the southern sky (Epcchtein et al. 1999). Data from the DENIS survey was cross correlated with the 2MASS data for regions near the Chamaeleon I dark cloud and near the Galactic Plane at a longitude of $\approx 323^\circ$ in order to find select stars that have large extinctions and correspondingly large near-infrared colors. No attempt was made to assess the spatial uniformity of the DENIS data and the color transformations across the sky. Using the data server at the Centre de Données astronomiques de Strasbourg, DENIS point sources were selected that had at least a signal to noise ratio of 15 in both the J and K_s bands with no error flags. DENIS sources were matched with 2MASS counterparts with a $5''$ search radius. Ten stars had 2MASS and DENIS K_s -band photometry that differed by more than 0.5^m and were omitted from the fit. The 2MASS and DENIS photometry for the 190 remaining stars is shown in Figure 7. The 2MASS and DENIS photometry are evidently correlated, but as indicated in Table 2, the reduced chi-squared from the linear fit is significantly greater than expected based on random noise. This may be a result from comparing photometry in crowded regions in the Galactic plane, which was necessary in order to identify red stars for the color transformations. The large reduced chi-squared values indicate that the uncertainties in the fitted parameters quoted below are underestimated, perhaps by as much as a $\approx \sqrt{2}$ given the value of χ^2_ν . The derived transformations are

$$(K_s)_{\text{2MASS}} = (K_s)_{\text{DENIS}} + (0.006 \pm 0.004)(J - K_s)_{\text{DENIS}} + (-0.024 \pm 0.006) \quad (16)$$

$$(J - K_s)_{\text{2MASS}} = (0.981 \pm 0.006)(J - K_s)_{\text{DENIS}} + (0.023 \pm 0.009) \quad (17)$$

$$(18)$$

4.5. ESO

The European Southern Observatory (ESO) photometric system was defined by Engels et al. (1981) and Wamsteker (1981) and later updated by Bouchet, Manfroid, & Schmider (1991) and van

der Bliek, Manfroid, & Bouchet (1996). Figure 8 compares the ESO and 2MASS photometry for 56 standards in van der Bliek, Manfroid, & Bouchet (1996) that have available 2MASS photometry. As seen in this figure, the range of near-infrared colors spanned by the available data is limited. The derived color transformations are

$$(K_s)_{\text{2MASS}} = K_{\text{ESO}} + (0.005 \pm 0.011)(J - K)_{\text{ESO}} + (-0.045 \pm 0.004) \quad (19)$$

$$(J - H)_{\text{2MASS}} = (0.983 \pm 0.030)(J - H)_{\text{ESO}} + (-0.049 \pm 0.008) \quad (20)$$

$$(J - K_s)_{\text{2MASS}} = (0.956 \pm 0.017)(J - K)_{\text{ESO}} + (-0.008 \pm 0.006) \quad (21)$$

$$(H - K_s)_{\text{2MASS}} = (0.956 \pm 0.126)(H - K)_{\text{ESO}} + (0.034 \pm 0.006) \quad (22)$$

4.6. LCO (Persson standards)

Persson et al. (1998) developed a grid of J , H , K , and K_s -band standards for the HST NICMOS camera using observations from the Las Campanas Observatory (LCO) in Chile. Included in the Persson list of standards are many of the red stars observed by Elias et al. (1983) in the CIT and AAO photometric systems. As discussed above, star cskf-13a in the Elias et al. (1983) list have been omitted. In addition, the 2MASS photometry for IRAS 537s differs from the Persson et al. (1998) photometry by up to 0.26^m, and L547 is a variable star (Persson et al. 1998). Excluding these three stars, 82 stars from Persson et al. (1998) have available 2MASS photometry at the time of this study. It should be noted that a Persson et al. (1998) standard has been adopted as the fiducial calibrator in 29 of the 35 2MASS calibration fields, thereby connecting the zero-points between the 2MASS and LCO photometric systems. A photometric offset of roughly zero, then, is expected in the 2MASS-LCO transformation equations, although not necessarily a unit slope. Indeed, as shown in Figure 9 for the LCO K -band data and Figure 10 for the LCO K_s -band data, the zero-point offset between the LCO and 2MASS photometry is approximately zero. The derived transformations for the LCO K and K_s band photometry are

$$(K_s)_{\text{2MASS}} = K_{\text{LCO}} + (-0.001 \pm 0.002)(J - K)_{\text{LCO}} + (-0.006 \pm 0.004) \quad (23)$$

$$(J - H)_{\text{2MASS}} = (0.995 \pm 0.006)(J - H)_{\text{LCO}} + (0.002 \pm 0.006) \quad (24)$$

$$(J - K_s)_{\text{2MASS}} = (1.013 \pm 0.005)(J - K)_{\text{LCO}} + (-0.007 \pm 0.006) \quad (25)$$

$$(H - K_s)_{\text{2MASS}} = (1.008 \pm 0.010)(H - K)_{\text{LCO}} + (0.002 \pm 0.005) \quad (26)$$

$$(K_s)_{\text{2MASS}} = (K_s)_{\text{LCO}} + (-0.002 \pm 0.002)(J - K_s)_{\text{LCO}} + (-0.010 \pm 0.004) \quad (27)$$

$$(J - K_s)_{\text{2MASS}} = (1.007 \pm 0.005)(J - K_s)_{\text{LCO}} + (0.002 \pm 0.006) \quad (28)$$

$$(H - K_s)_{\text{2MASS}} = (1.019 \pm 0.010)(H - K_s)_{\text{LCO}} + (0.005 \pm 0.005) \quad (29)$$

4.7. MSSSO

McGregor (1994) presented standard star photometry for the Mount Stromlo and Siding Spring Observatory (MSSSO), which is nearly identical to the Mount Stromlo Observatory (MSO) photometric system described by Jones & Hyland (1982). In addition, McGregor (1994) report photometry in the MSSSO system for a number of red stars. These stars were included when deriving the color transformations in order to increase the accuracy of the transformations. Star cskf-13a was excluded from this analysis as already noted, as well as the stars from Jones & Hyland (1980) as they are located in crowded regions in the Galactic Plane. Figure 11 compares the MSSSO and 2MASS photometry for the 20 stars from McGregor (1994) used in the analysis. The derived color transformations are

$$(K_s)_{\text{2MASS}} = K_{\text{MSSSO}} + (-0.021 \pm 0.006)(J - K)_{\text{MSSSO}} + (-0.023 \pm 0.008) \quad (30)$$

$$(J - H)_{\text{2MASS}} = (0.991 \pm 0.014)(J - H)_{\text{MSSSO}} + (-0.010 \pm 0.014) \quad (31)$$

$$(J - K_s)_{\text{2MASS}} = (1.005 \pm 0.008)(J - K)_{\text{MSSSO}} + (0.011 \pm 0.011) \quad (32)$$

$$(H - K_s)_{\text{2MASS}} = (1.037 \pm 0.029)(H - K)_{\text{MSSSO}} + (0.019 \pm 0.012) \quad (33)$$

4.8. SAAO

Carter (1990) updated the South Africa Astronomical Observatory (SAAO) photometric system originally defined by Glass (1974) and later extended the standard star list to fainter magnitudes (Carter & Meadows 1995). Figure 12 compares the SAAO and 2MASS photometry for 94 stars. Most of the relatively blue stars are from the list of $K \approx 8$ standards in Carter & Meadows (1995), while the stars with red colors are predominantly from Carter (1990). The derived transformations are

$$(K_s)_{\text{2MASS}} = K_{\text{SAAO}} + (0.020 \pm 0.007)(J - K)_{\text{SAAO}} + (-0.025 \pm 0.004) \quad (34)$$

$$(J - H)_{\text{2MASS}} = (0.949 \pm 0.018)(J - H)_{\text{SAAO}} + (-0.054 \pm 0.006) \quad (35)$$

$$(J - K_s)_{\text{2MASS}} = (0.940 \pm 0.010)(J - K)_{\text{SAAO}} + (-0.011 \pm 0.005) \quad (36)$$

$$(H - K_s)_{\text{2MASS}} = (0.961 \pm 0.036)(H - K)_{\text{SAAO}} + (0.040 \pm 0.005) \quad (37)$$

4.9. UKIRT

The standard star photometry for the United Kingdom Infrared Telescope (UKIRT) was first established by Casali & Hawarden (1992) and extended by Hawarden et al. (2000). Three of the 2MASS calibration fields include five UKIRT standards (FS4, FS13, and FS15-17; Nikolaev

et al. 2000). The UKIRT photometric system is being replaced by the Mauna Kea Observatory near-infrared photometric system, which is a result of a coordinated effort by several observatories to use a consistent set of filters. Fundamental photometry of the standard stars in this new photometric system was not available at the time of this study. Therefore, the color transformations between the UKIRT and 2MASS photometric systems are derived here, and the most recent transformations between the UKIRT and Mauna Kea Observatory systems can be found in Hawarden et al. (2000).

Star FS18 was omitted from the linear fit since it is a unresolved double system at the resolution of 2MASS with $1.38''$ resolution (Hawarden et al. 2000). Also, the 2MASS J -band photometry for FS142 and FS143 differ from the UKIRT magnitudes by $+0.30$ magnitudes and -0.42 magnitudes respectively, although the H and K_s magnitudes are not significantly discrepant. Both stars are located in the Serpens star forming region and have $(J - K_s)$ colors between 2.5 and 3.5 magnitudes, and one (FS142, also known as EC51) is a possible variable star (Kaas 1999). It is unclear then if the J -band magnitudes for these two stars is a result of low signal to noise (< 10) in the 2MASS data, or if these are variable stars. Both objects were removed from the fit. Figure 13 compares the UKIRT and 2MASS photometry for 72 stars. The derived transformations are

$$(K_s)_{\text{2MASS}} = K_{\text{UKIRT}} + (0.004 \pm 0.006)(J - K)_{\text{UKIRT}} + (0.002 \pm 0.004) \quad (38)$$

$$(J - H)_{\text{2MASS}} = (1.069 \pm 0.015)(J - H)_{\text{UKIRT}} + (-0.027 \pm 0.007) \quad (39)$$

$$(J - K_s)_{\text{2MASS}} = (1.069 \pm 0.011)(J - K)_{\text{UKIRT}} + (-0.012 \pm 0.006) \quad (40)$$

$$(H - K_s)_{\text{2MASS}} = (1.062 \pm 0.027)(H - K)_{\text{UKIRT}} + (0.017 \pm 0.005) \quad (41)$$

5. Summary

Colors and magnitudes of stars observed in the AAO, ARNICA, CIT, DENIS, ESO, LCO, MSSSO, SAAO, and UKIRT photometric systems are compared to photometry from the 2MASS survey. These data have been used to derive the K -band, $J - H$, $J - K$, and $H - K$ color transformations from these systems to the photometric system implicit to the 2MASS Second Incremental Data Release. The transformation equations for the Bessell & Brett (1988) and Koornneef (1983) homogenized photometric systems have been derived indirectly by first transforming their results to the CIT and SAAO systems respectively, and then to the 2MASS system. The range of colors that these transformation equations are valid over is set by the published photometry and can be determined through inspection of Figures 3-14.

JMC would like to thank Mike Skrutskie for many useful suggestions throughout the course of this work. He also thanks Roc Cutri, Sandy Leggett, Jay Elias, and the anonymous referee for their comments on this paper, and Bill Wheaton and Martin Cohen for their assistance in obtaining the data for the filter transmissions and atmospheric models. This publication makes use of data prod-

ucts from the Two Micron All Sky Survey, which is a joint project of the University of Massachusetts and the Infrared Processing and Analysis Center, funded by the National Aeronautics and Space Administration and the National Science Foundation. 2MASS science data and information services were provided by the InfraRed Science Archive (IRSA) at IPAC. This research has made use of the SIMBAD database, operated at CDS, Strasbourg, France. JMC acknowledges support from Long Term Space Astrophysics Grant NAG5-8217 and the Owens Valley Radio Observatory, which is supported by the National Science Foundation through NSF grant number AST-9981546.

A. Bessell & Brett Homogenized System

Bessell & Brett (1988) present a homogenized photometric system based largely on the SAAO observations from Glass (1974). The Glass (1974) standard stars are saturated in the 2MASS images and cannot be tied directly to the 2MASS photometric system. However, the Bessell & Brett (1988) and 2MASS photometric systems can be related indirectly using the transformations derived here and those listed in Bessell & Brett (1988). In particular, the CIT transformation equations were used since they have been derived using stars that span a large range of near-infrared colors. Formally, the transformation between the K magnitude measured in the CIT system and the Bessell & Brett (1988) homogenized system contains a weak dependence on the $V - K$ stellar color. This term was not included in deriving the following transformations:

$$(K_s)_{\text{2MASS}} = K_{\text{BB}} + (0.000 \pm 0.005)(J - K)_{\text{BB}} + (-0.044 \pm 0.003) \quad (\text{A1})$$

$$(J - H)_{\text{2MASS}} = (0.980 \pm 0.009)(J - H)_{\text{BB}} + (-0.045 \pm 0.006) \quad (\text{A2})$$

$$(J - K_s)_{\text{2MASS}} = (0.972 \pm 0.006)(J - K)_{\text{BB}} + (-0.011 \pm 0.005) \quad (\text{A3})$$

$$(H - K_s)_{\text{2MASS}} = (0.996 \pm 0.019)(H - K)_{\text{BB}} + (0.028 \pm 0.005) \quad (\text{A4})$$

B. Koornneef Homogenized System

Koornneef (1983) present an homogenized photometric system that is a hybrid of the Johnson (Johnson et al. 1966) and SAAO (Glass 1974) systems. Nearly all of the standard stars listed in Koornneef (1983) are saturated in the 2MASS data, and transformations to the 2MASS photometric system could not be derived directly. However, a number of stars in Koornneef (1983) were also observed by Carter (1990) in the SAAO system, and can be used to tie the Koornneef (1983) system to 2MASS using the results from Section 4.8. Figure 14 compares the Carter (1990) and Koornneef (1983) photometry for 133 stars in common between the two studies. An uncertainty of 0.02^m was assumed for the Koornneef (1983) photometry in performing the linear fit using the FITEXY routine (Press et al. 1992). The derived color transformations between the two systems are

$$K_{\text{SAAO}} = K_{\text{Koornneef}} + (0.018 \pm 0.008)(J - K)_{\text{Koornneef}} + (-0.022 \pm 0.004) \quad (\text{B1})$$

$$(J - H)_{\text{SAAO}} = (1.079 \pm 0.014)(J - H)_{\text{Koornneef}} + (0.010 \pm 0.006) \quad (\text{B2})$$

$$(J - K)_{\text{SAAO}} = (1.032 \pm 0.011)(J - K)_{\text{Koornneef}} + (-0.006 \pm 0.006) \quad (\text{B3})$$

$$(H - K)_{\text{SAAO}} = (0.824 \pm 0.050)(H - K)_{\text{Koornneef}} + (-0.014 \pm 0.006) \quad (\text{B4})$$

Using the 2MASS-SAAO results from Section 4.8, the color transformations between the Koornneef (1983) and 2MASS systems are

$$(K_s)_{\text{2MASS}} = K_{\text{Koornneef}} + (0.039 \pm 0.019)(J - K)_{\text{Koornneef}} + (-0.047 \pm 0.006) \quad (\text{B5})$$

$$(J - H)_{\text{2MASS}} = (1.024 \pm 0.024)(J - H)_{\text{Koornneef}} + (-0.045 \pm 0.006) \quad (\text{B6})$$

$$(J - K_s)_{\text{2MASS}} = (0.970 \pm 0.015)(J - K)_{\text{Koornneef}} + (-0.017 \pm 0.005) \quad (\text{B7})$$

$$(H - K_s)_{\text{2MASS}} = (0.792 \pm 0.056)(H - K)_{\text{Koornneef}} + (0.027 \pm 0.005) \quad (\text{B8})$$

REFERENCES

Allen, D. A. & Cragg, T. A. 1983, MNRAS, 203, 777

Bessell, M. S., & Brett, J. M. 1988, PASP, 100, 1134

Bouchet, P., Manfroid, J., & Schmider, F. X. 1991, A&AS, 91, 409

Carter, B. S. 1990, MNRAS, 242, 1

Carter, B. S. & Meadows, V. S. 1995, MNRAS, 276, 734

Casali, M., & Hawarden, T. 1992, The UKIRT/JCMT Newsletter, No. 4, 33

Cutri, R. M. et al. 2000, Explanatory Supplement to the 2MASS Second Incremental Data Release,
<http://www.ipac.caltech.edu/2mass/releases/second/doc/explsup.html>

Elias, J. H., Frogel, J. A., Hyland, A. R., & Jones, T. J. 1993, AJ, 88, 1027

Elias, J. H., Frogel, J. A., Matthews, K., & Neugebauer, G. 1982, AJ, 87, 1029

Engels, D., Sherwood, W. A., Wamsteker, W., & Schultz, G. V. 1981, A&AS, 45, 5

Epcstein, N. et al. 1999, A&A, 349, 236

Frogel, J. A., Persson, S. E., Aaronson, M., & Matthews, K. 1978, ApJ, 220, 75

Glass, I. S. 1974, Mon. Notes Astron. Soc. South Africa, 33, 53

Hawarden, T., et al. 2000, in preparation; see also UKIRT web site at
http://www.jach.hawaii.edu/JACpublic/UKIRT/astronomy/calib/faint_stds.html

Hunt, L. K., Mannucci, F., Testi, L., Migliorini, S., Stanga, R. M., Baffa, C., Lisi, F., & Vanzi, L. 1998, AJ, 115, 2594

_____. 2000, AJ, 119, 985

Isobe, T., Feigelson, E. D., Akritas, M. G., & Basu, G. J. 1990, ApJ, 364, 104

Johnson, H. L. Mitchell, R. I., Iriarte, B., & Wisniewski, W. Z. 1966, Comm. Lunar. and Planetary Lab. 4, 99

Jones, T. J., & Hyland, A. R. 1980, MNRAS, 192, 359

_____. 1982, MNRAS, 200, 509

Kaas, A. A. 1999, AJ, 118, 558

Koornneef, J. 1983, A&AS, 51, 489

Table 1. Photometric Systems

System	Reference	Nstars
AAO	Allen & Cragg 1983	4
	Elias et al. 1983	10
ARNICA	Hunt et al. 1988	65
CIT	Elias et al. 1982	33
	Elias et al. 1983	8
DENIS	Epchtein et al. 1999	190
ESO	van der Bliek et al. 1996	56
LCO	Persson et al. 1998	82
MSSSO	McGregor 1994	20
SAAO	Carter 1990	29
	Carter & Meadows 1995	65
UKIRT	Hawarden et al. 2000	72

Table 2. Goodness-of-Fit Parameters

System	χ^2_ν				q			
	K	$J - H$	$J - K$	$H - K$	K	$J - H$	$J - K$	$H - K$
AAO	1.6	0.4	1.2	0.8	0.08	0.95	0.26	0.68
ARNICA	1.1	0.5	0.5	0.5	0.36	1.00	1.00	1.00
CIT	1.8	0.9	1.3	0.8	0.002	0.60	0.10	0.84
DENIS	2.4	—	2.0	—	5×10^{-23}	—	5×10^{-15}	—
ESO	1.6	0.8	1.1	0.8	0.003	0.82	0.33	0.80
Koornneef ^a	0.5	0.2	0.2	0.1	0.99	1.00	1.00	1.00
LCO (K)	1.2	0.5	0.8	0.8	0.16	1.00	0.88	0.95
LCO (K_s)	0.7	—	0.6	0.5	0.99	—	1.00	1.00
MSSSO	1.6	0.4	0.7	0.7	0.05	0.99	0.79	0.84
SAAO	0.8	0.5	0.6	0.5	0.85	1.00	1.00	1.00
UKIRT	1.2	0.5	0.5	0.4	0.15	1.00	1.00	1.00

^aGoodness-of-fit-results are for the SAAO vs. Koornneef fit described in Appendix B.

McGregor, P. J. 1994, PASP, 106, 508

Nikolaev, S., Weinberg, M. D., Skrutskie, M. F., Cutri, R. M., Wheelock, S. L., Gizis, J. E., & Howard, E. M. 2000, AJ, 120, 3340

Persson, S. E., Murphy, D. C., Krzeminski, W., Roth, M., & Rieke, M. J. 1998, AJ, 116, 2475

Press, W. H., Teukolsky, S. A., Vetterling, W. T., & Flannery, B. P. 1992, Numerical Recipes in C Second Edition, (London:Cambridge Press)

van der Bliek, N. S., Manfroid, J., & Bouchet, P. 1996, A&AS, 119, 547

Wamsteker, W. 1981, A&A, 97, 329

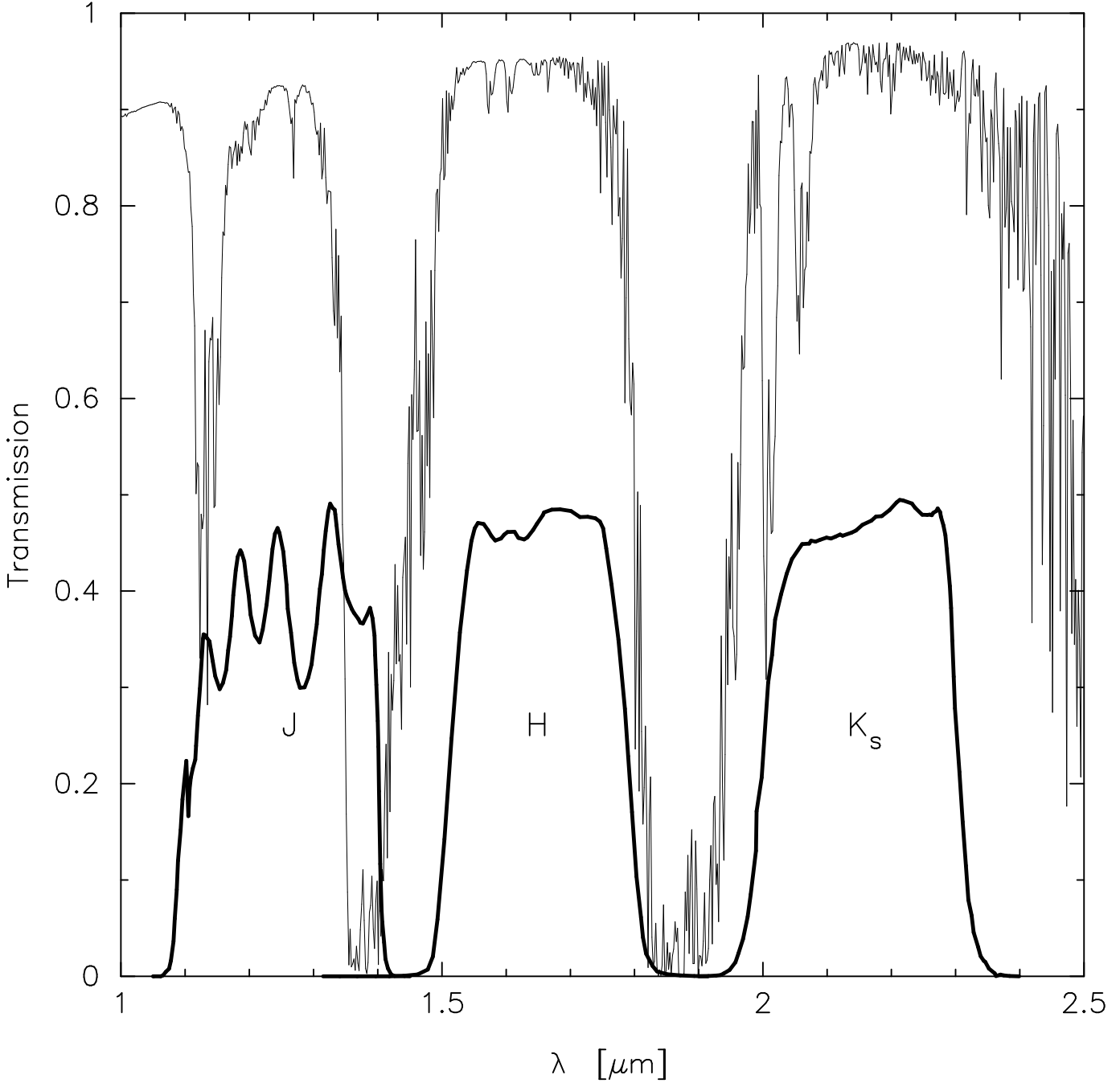


Fig. 1.— Transmission curves for the 2MASS optical path (thick solid curves), including the telescope mirror reflectivity, dewar window, anti-reflection coatings, dichroics, filters, and the NICMOS detector quantum efficiency, but excluding atmospheric absorption. The thin solid line shows the model atmospheric transmission for the mean observing conditions at Mt. Hopkins computed using the USAF PLEXUS code and binned to a resolution of $0.002\mu\text{m}$.

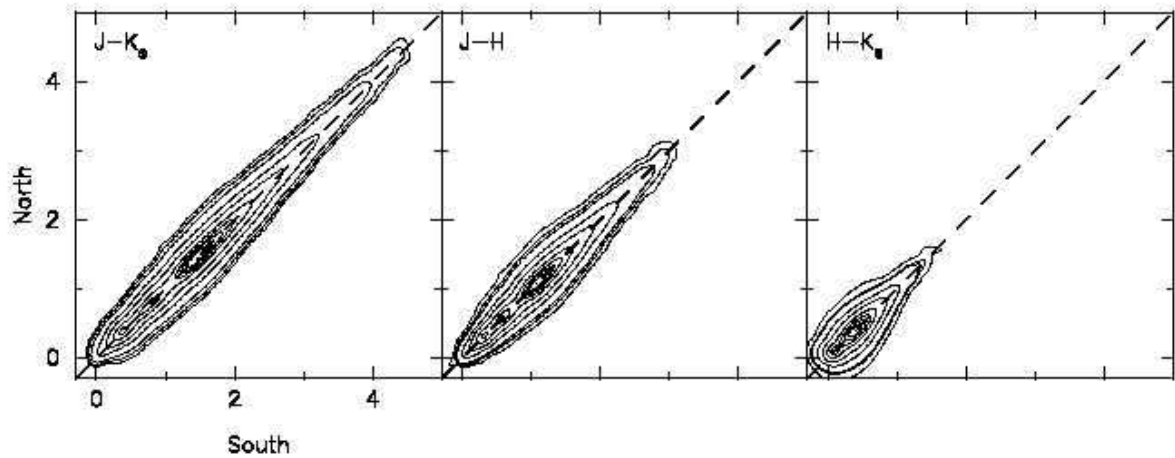


Fig. 2.— Comparison of the $J - K_s$, $J - H$, and $H - K_s$ colors for stars that have been observed by both the 2MASS northern and southern survey telescopes. The density plots were generated by representing each star with a gaussian kernel with a dispersion corresponding to the photometric errors. The contours are at levels of 0.01%, 0.1%, 1%, 5%, 20%, and increments of 20% thereafter of the peak density. The dashed line shows the expected relation if the two colors are equal.

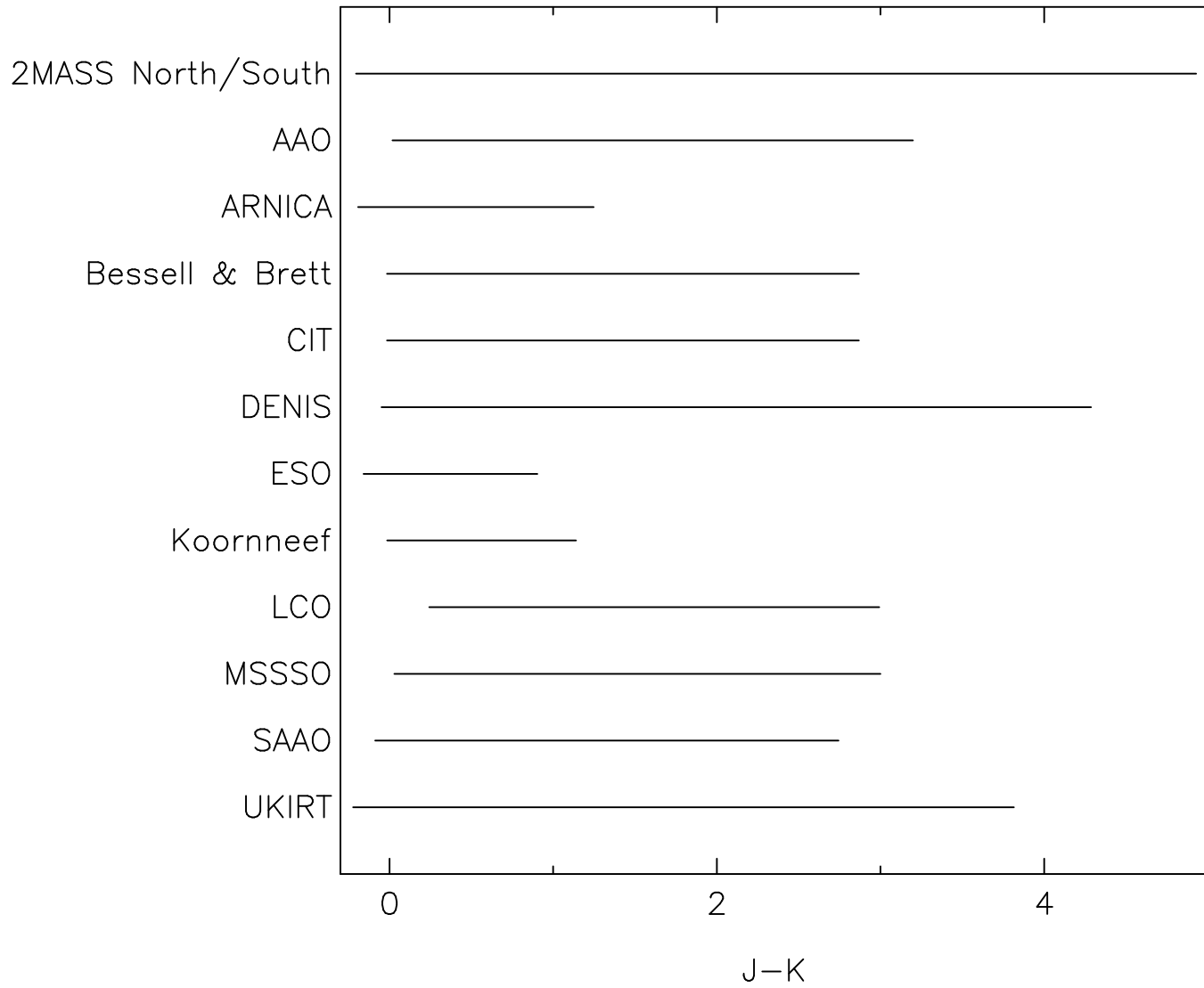


Fig. 3.— The range of observed $J - K$ colors spanned by the data for the various photometric systems analyzed here. The 2MASS North/South colors refer to the comparison of the 2MASS North and South photometry discussed in Section 3. The color transformations presented in this paper are not necessarily valid outside the $J - K$ colors shown in this figure. The appropriate limits for the $J - H$ and $H - K$ transformation equations can be obtained from inspection of Figures 4-12.

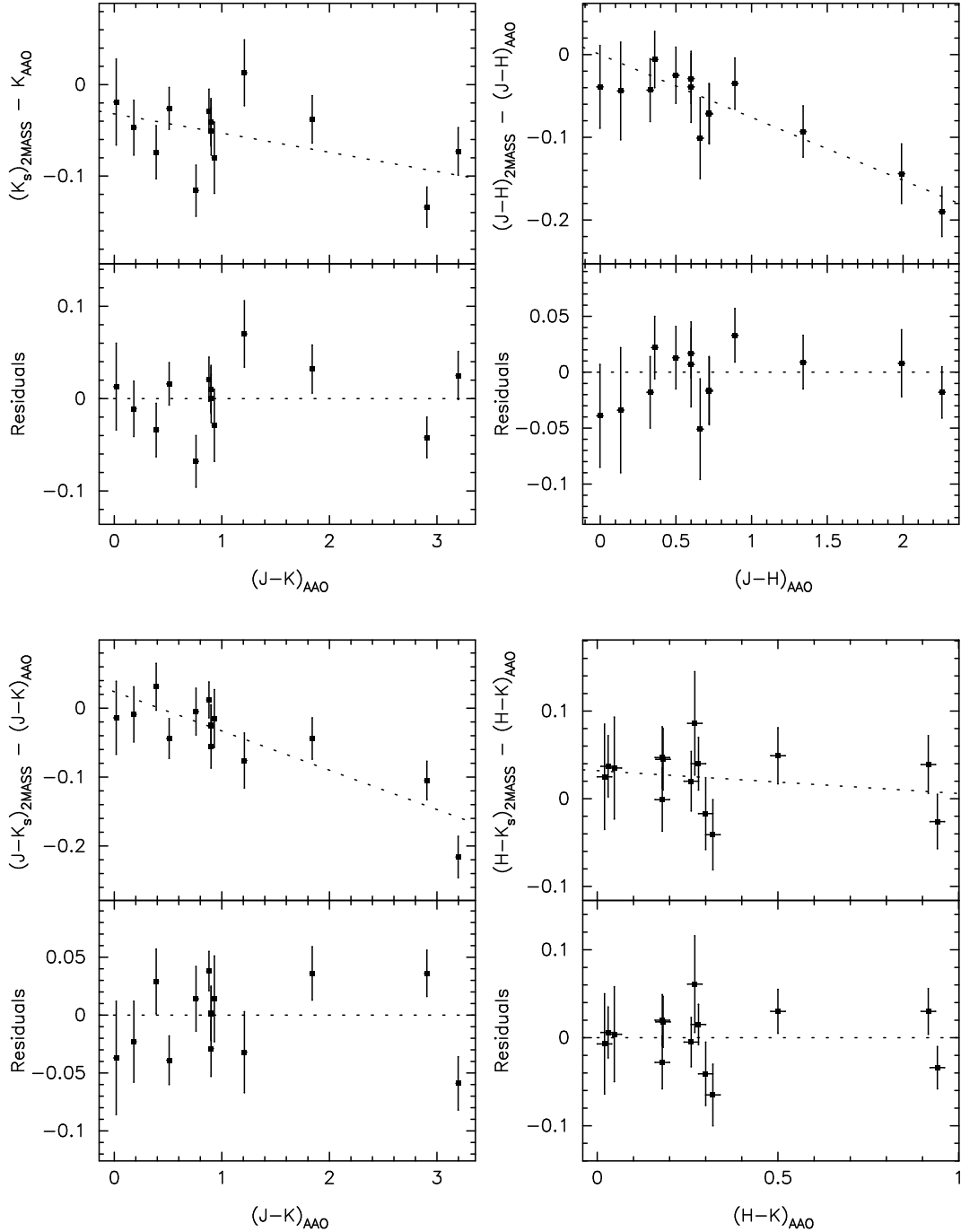


Fig. 4.— Comparison of the photometry of stars observed by Allen & Cragg (1983) and Elias et al. (1983) in the AAO photometric system that have available 2MASS photometry. The vertical and horizontal bars indicate the 1σ photometric uncertainties, although the AAO uncertainties are often smaller than the symbol size given the dynamic range along the X-axis. The upper left panel plots the difference in the K -band magnitudes as a function of the AAO $J - K$ color, and the remaining panels directly compare the $J - H$, $J - K$, and $H - K$ colors. The dotted line in the upper portion of each panel shows the derived transformation between the AAO and 2MASS photometric systems. The bottom portion of each panel shows the residuals from the fit, where the horizontal dotted line at zero is drawn for reference.

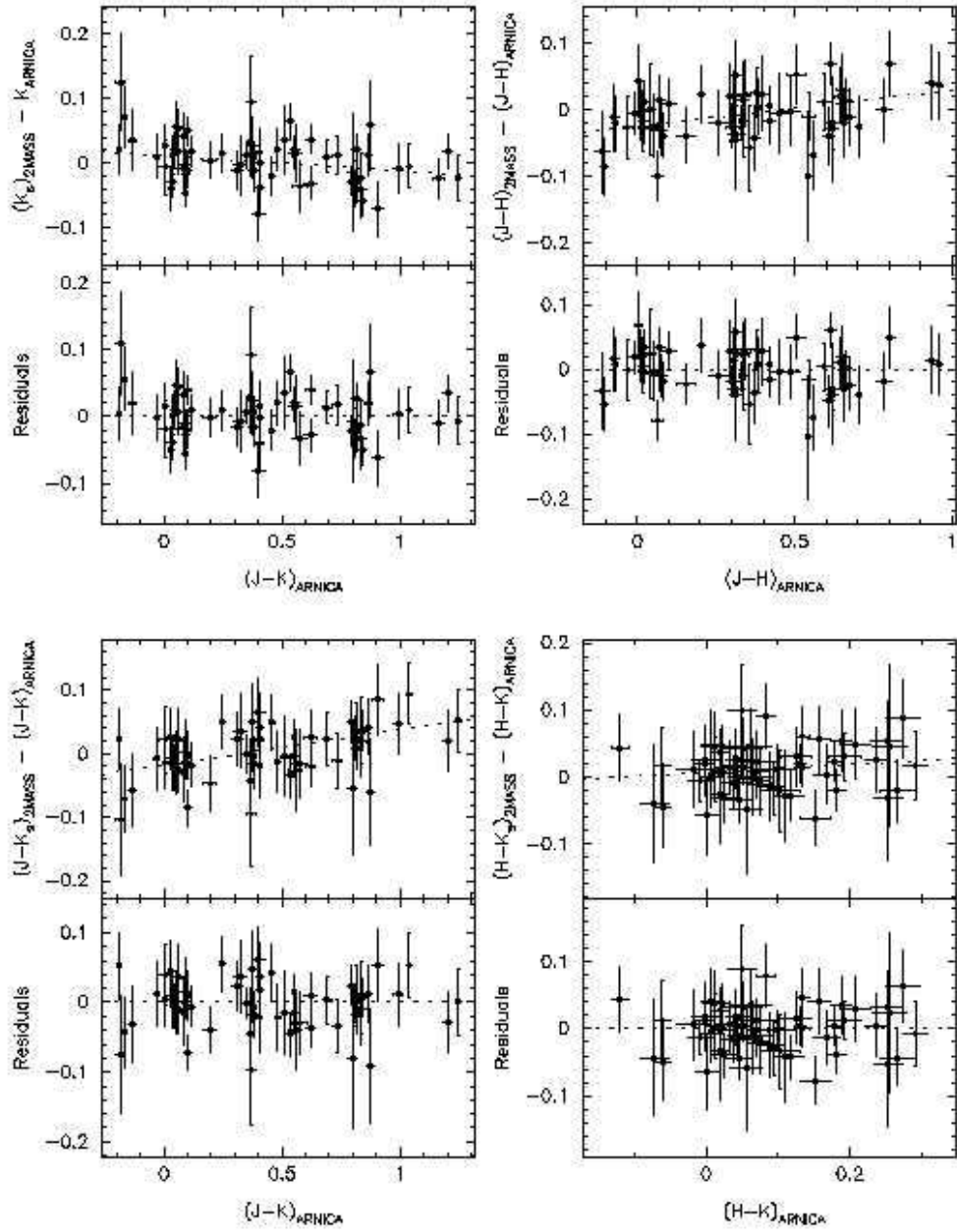


Fig. 5.— Same as Figure 4, except for the ARNICA photometric system. The ARNICA standard star photometry is from Hunt et al. (1998).

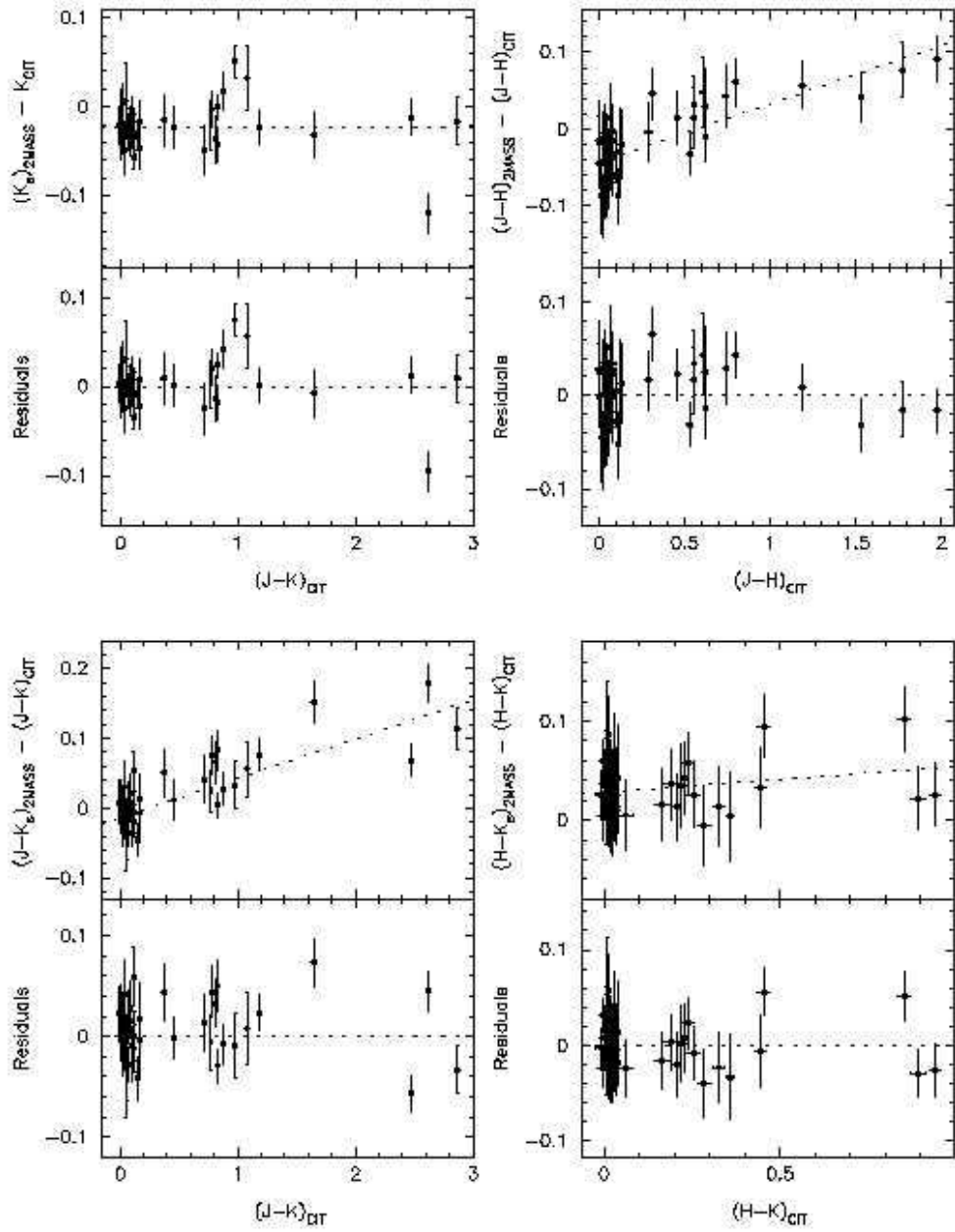


Fig. 6.— Same as Figure 4, except for the CIT photometric system. The CIT photometry is from Elias et al. (1982) and Elias et al. (1983).

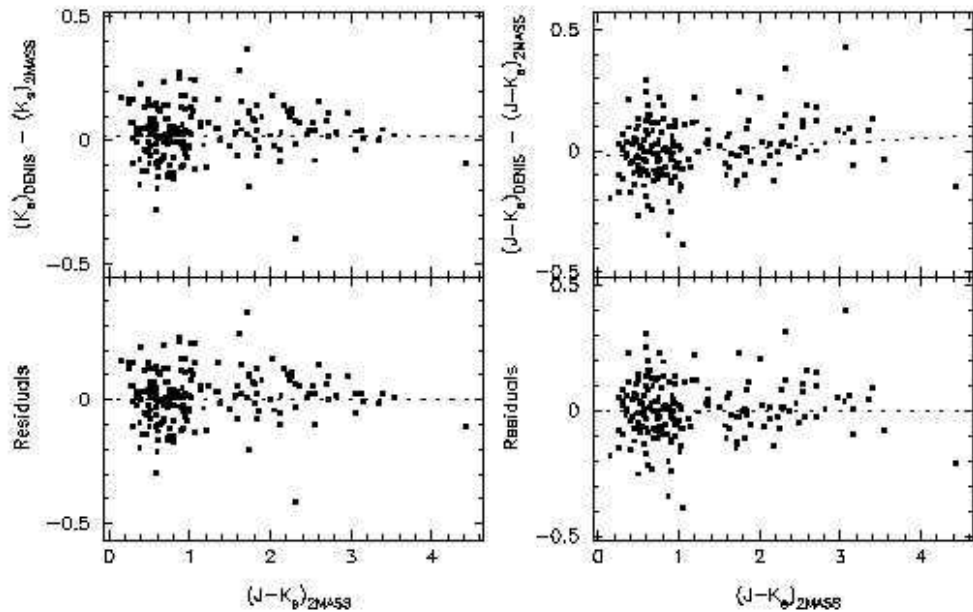


Fig. 7.— Same as Figure 4, except for the DENIS photometric system. Note that unlike other comparisons to published photometry presented here, the correlations are plotted as a function of the 2MASS photometry. The error bars for the individual points have been omitted for clarity. The DENIS photometry is from the DENIS preliminary data release described by Epchtein et al. (1999).

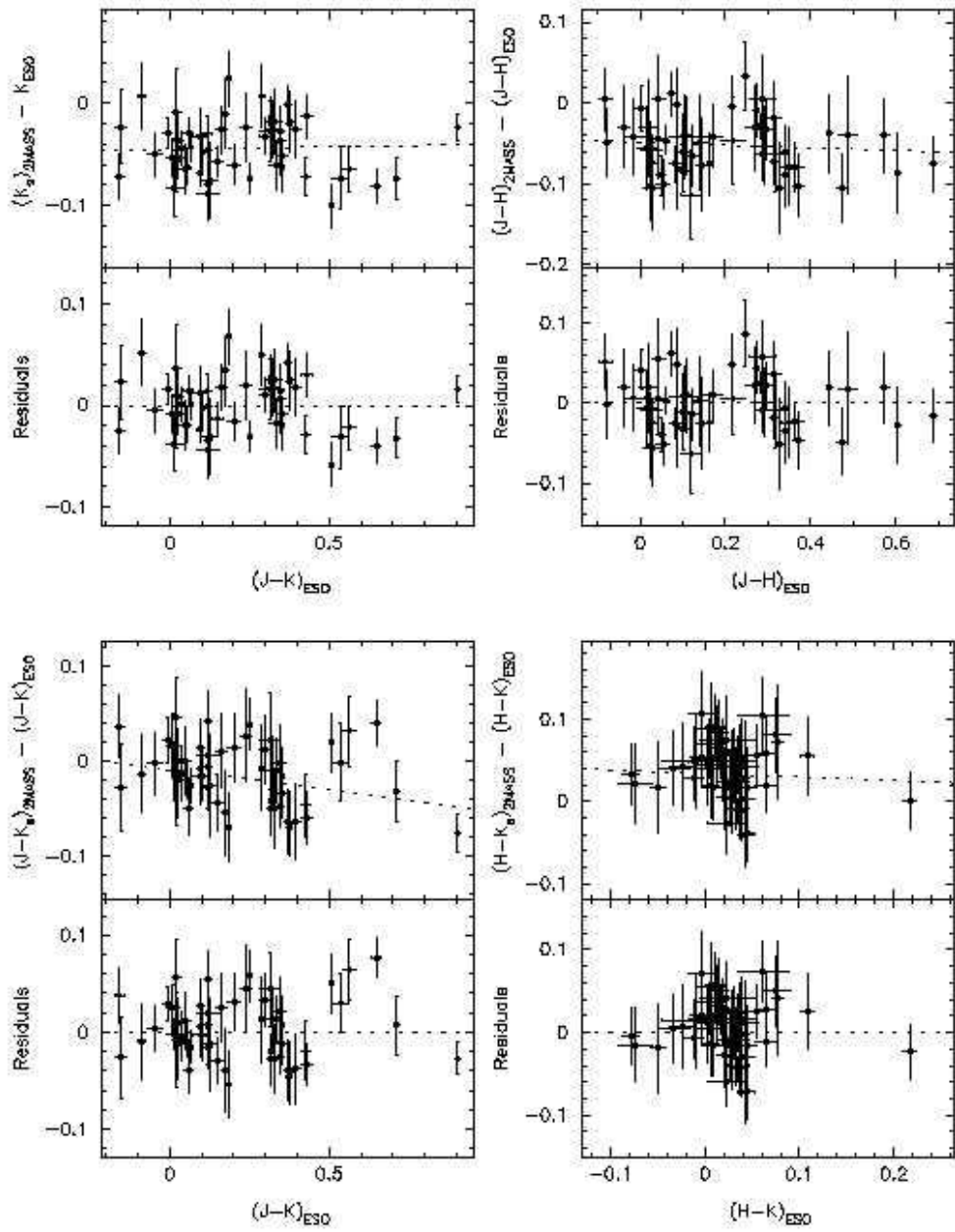


Fig. 8.— Same as Figure 4, except for the ESO photometric system. The ESO standard star photometry is from van der Bliek, Manfroid, & Bouchet (1996).

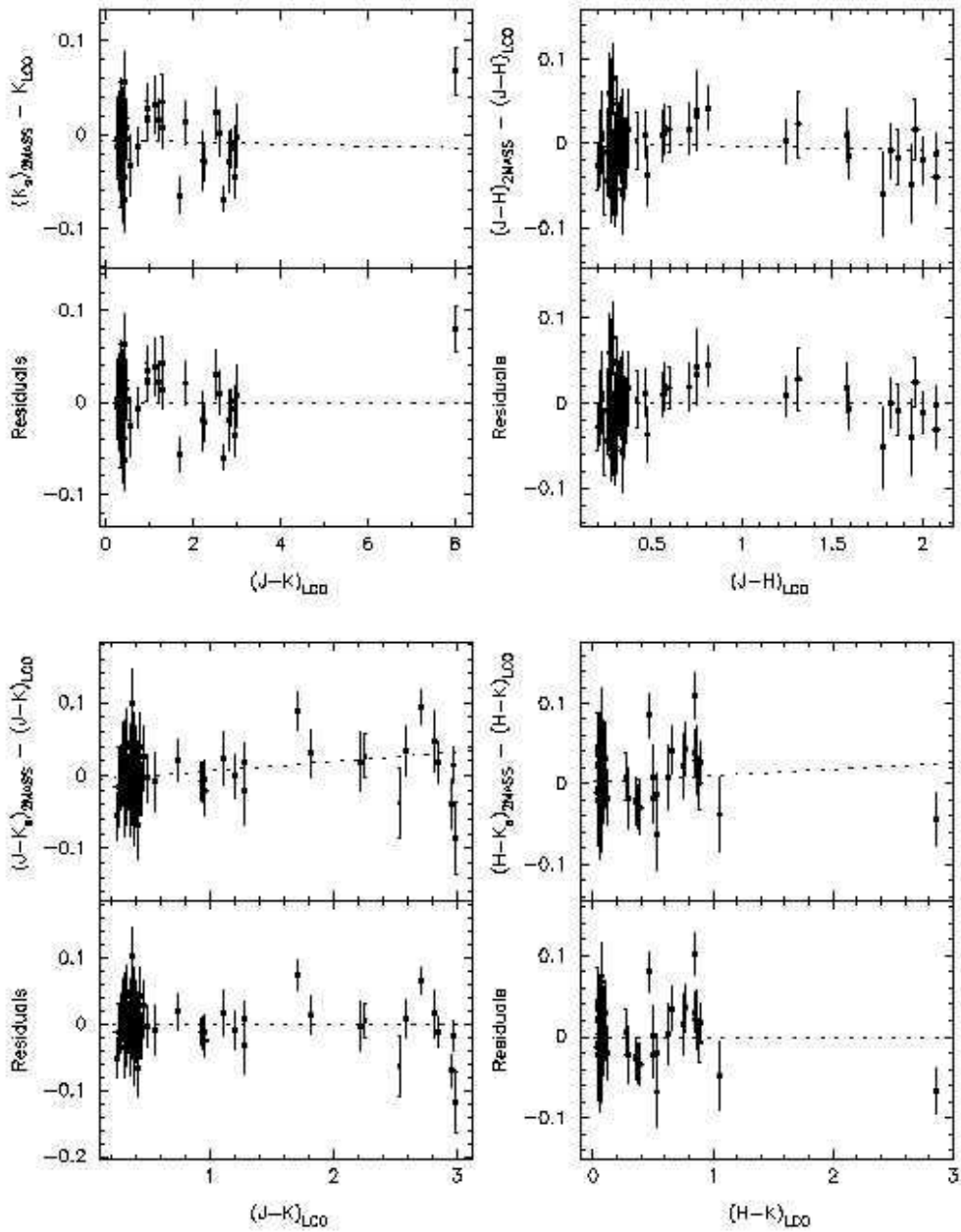


Fig. 9.— Same as Figure 4, except for the LCO photometric system with the K -band photometry as summarized in Persson et al. (1998). Comparison to the LCO K_s -band photometry is provided in Figure 10.

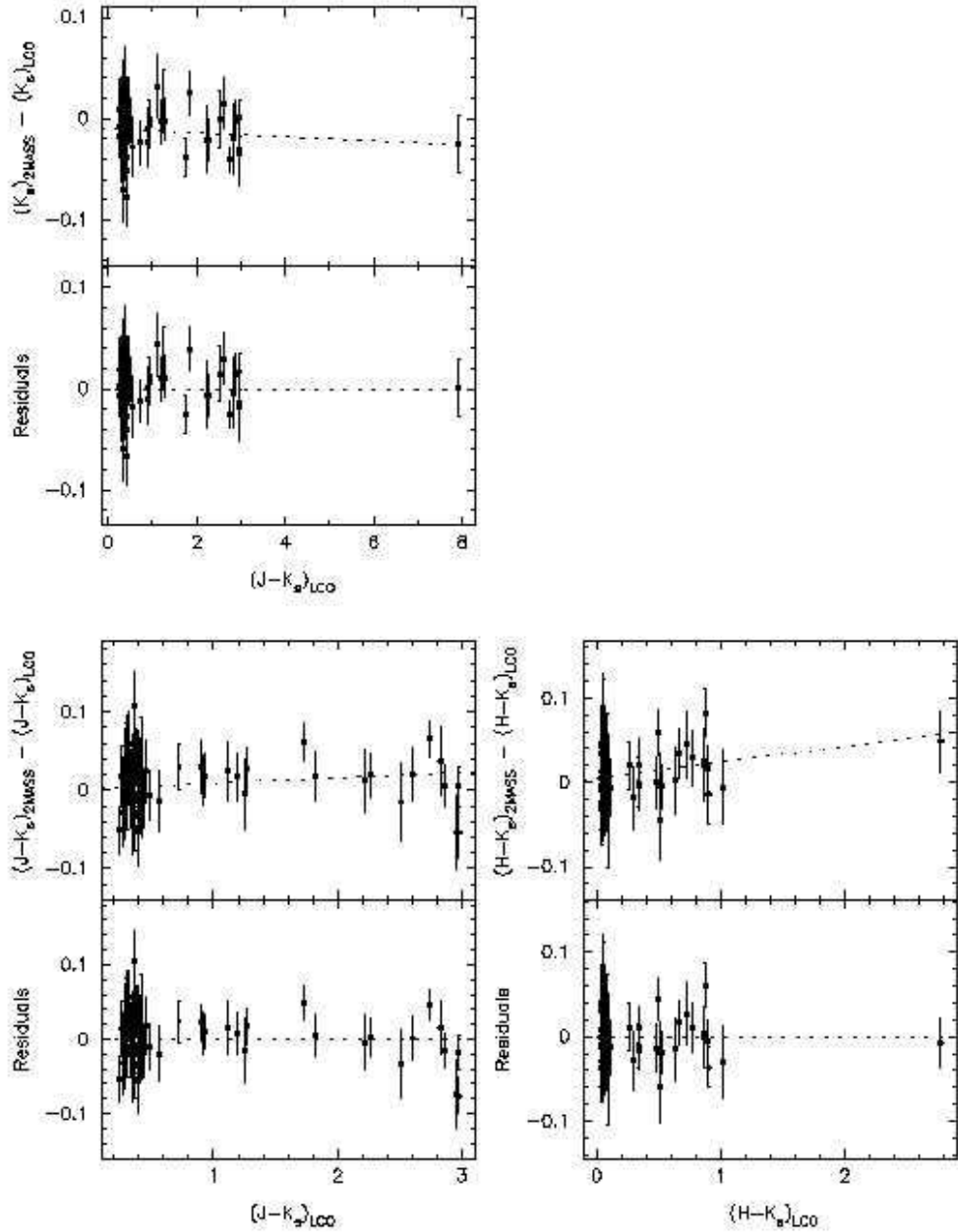


Fig. 10.— Same as Figure 4, except for the LCO (Persson) photometric system with the K_s -band photometry as summarized in Persson et al. (1998). The $J - H$ data for the LCO system and comparison of the LCO K -band photometry with 2MASS are shown in Figure 9.

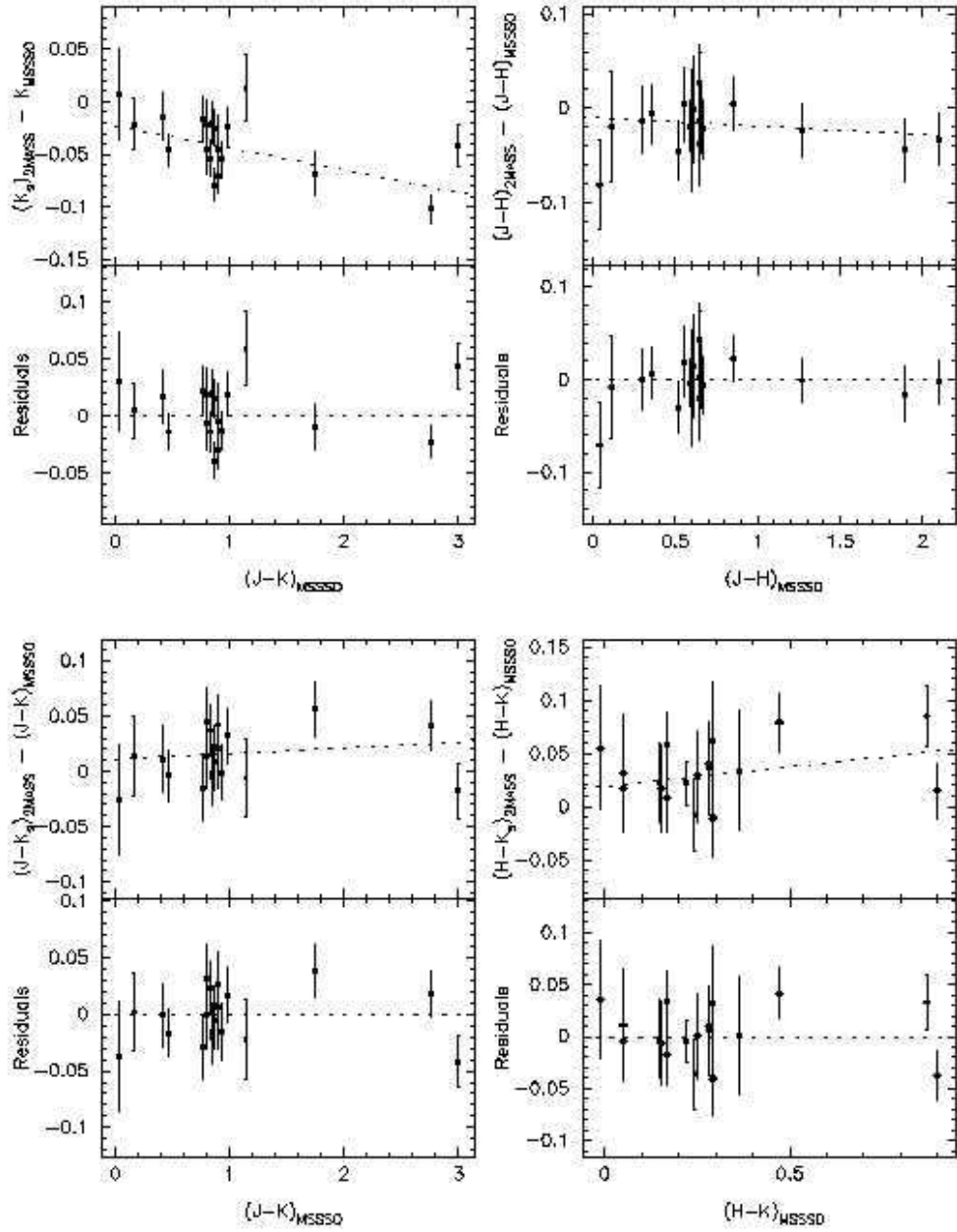


Fig. 11.— Same as Figure 4, except for the MSSSO photometric system. The MSSSO photometry is from McGregor (1994).

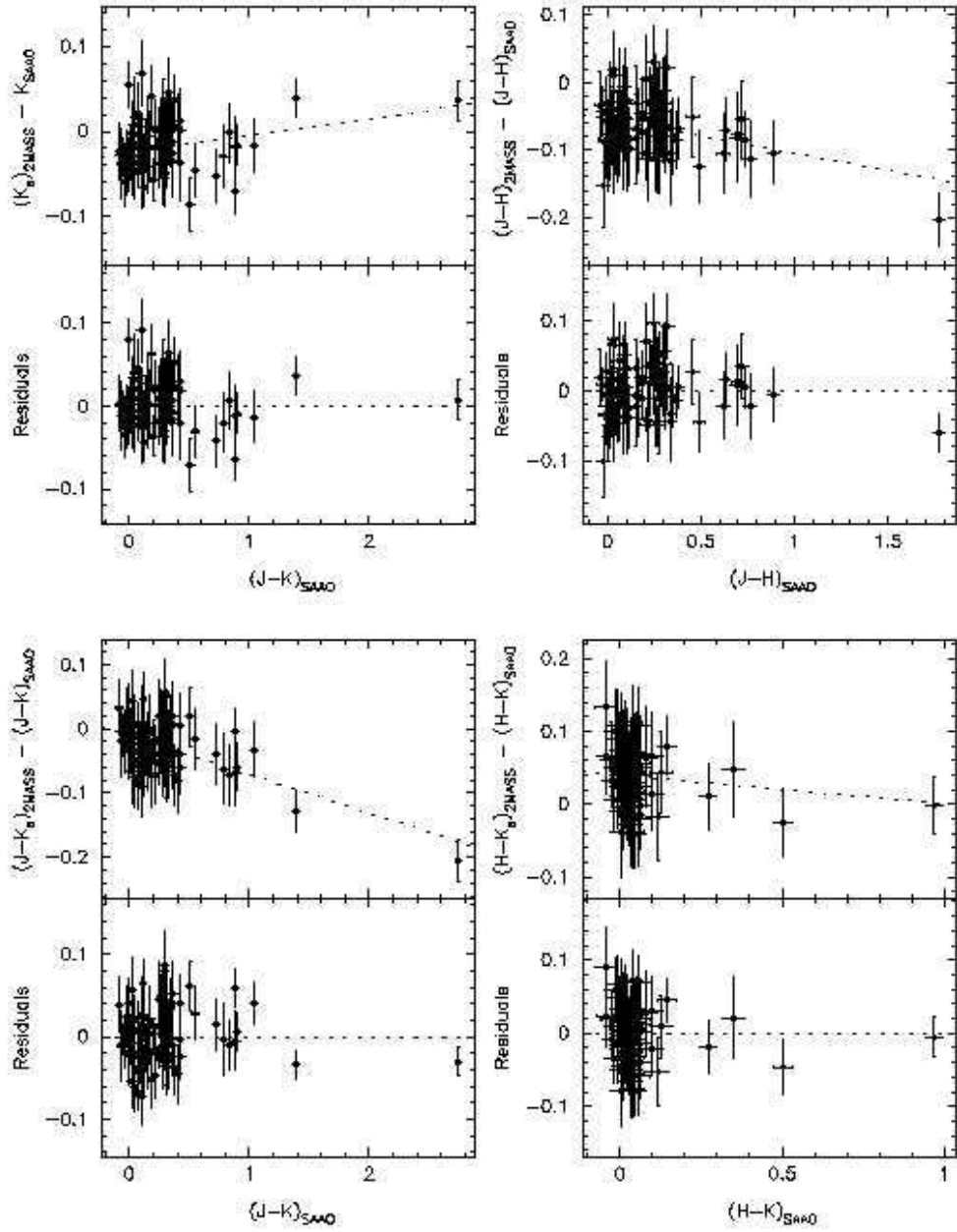


Fig. 12.— Same as Figure 4, except for the SAAO photometric system. The SAAO photometry is from Carter (1990) and Carter & Meadows (1995).

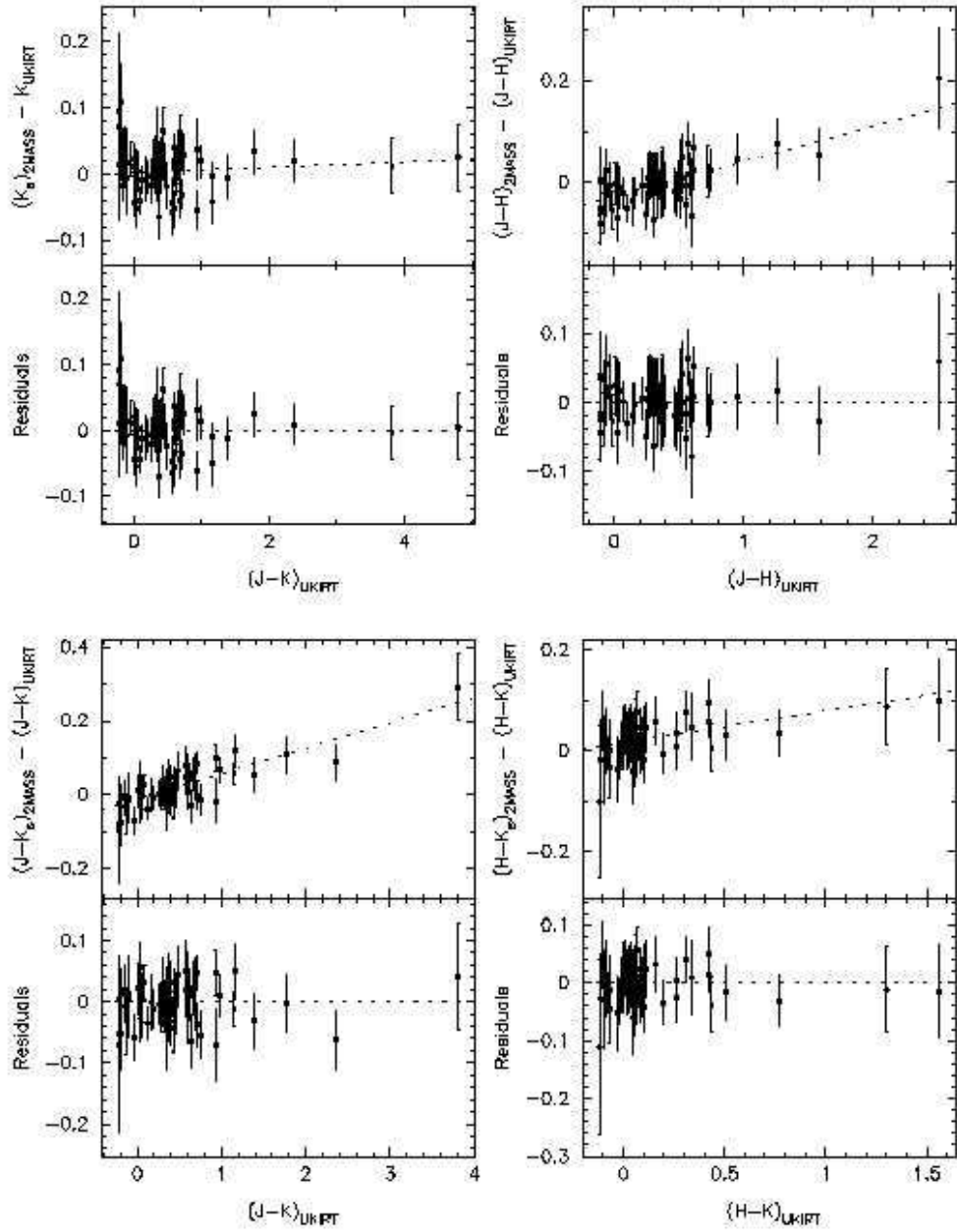


Fig. 13.— Same as Figure 4, except for UKIRT photometric system. The UKIRT standard star photometry is from Hawarden et al. (2000, see also Casali & Hawarden 1992).

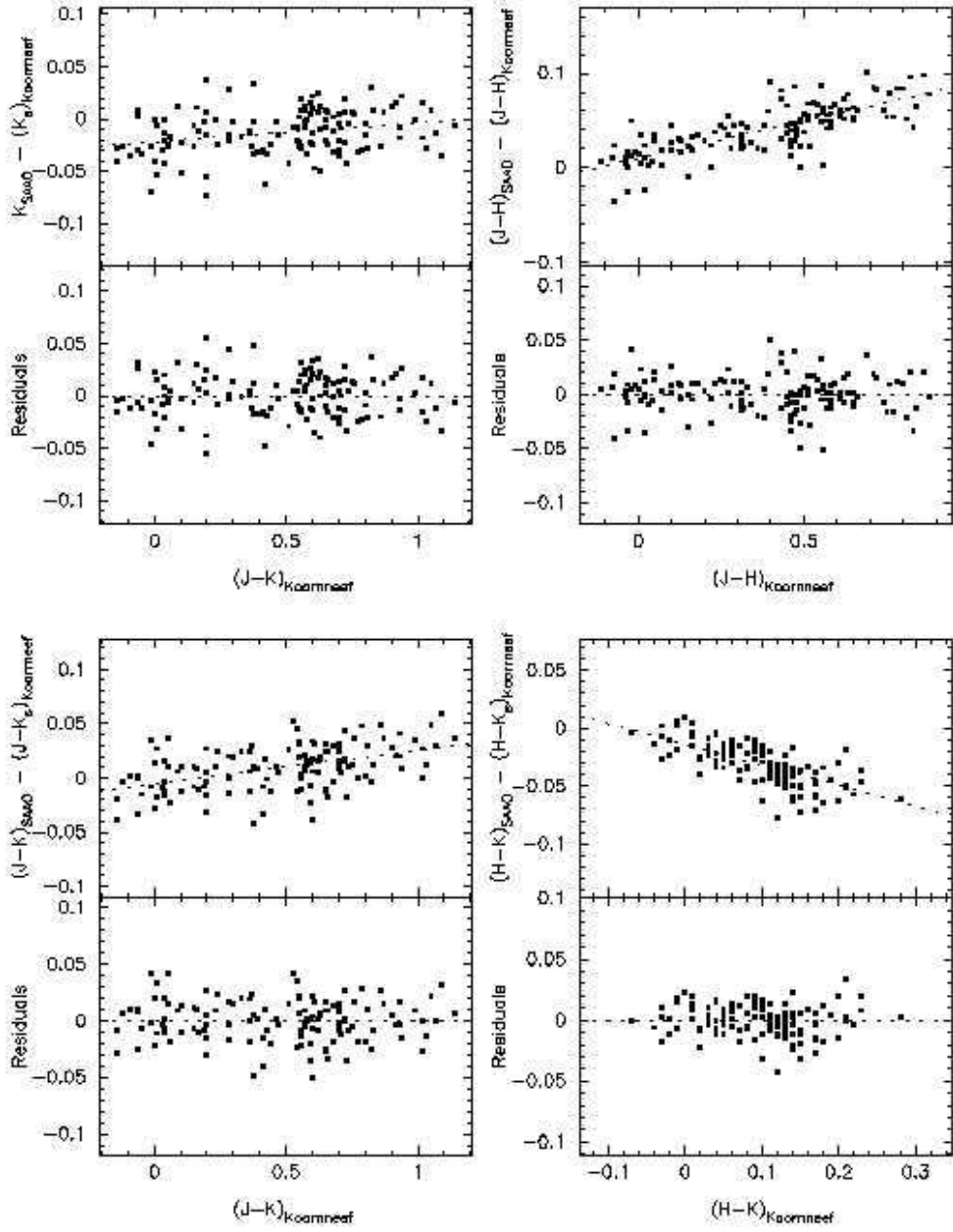


Fig. 14.— Comparison of the photometry for 133 stars in common between Carter (1990) and Koornneef (1983). The error bars for the individual points have been omitted for clarity. These results were used in combination with the 2MASS-SAAO color transformations derived in Section 4.8 to determine indirectly the transformations between the Koornneef (1983) homogenized photometric system and 2MASS.